Solvent Extraction Research and Development, Japan, **Vol. 21, No 2, 147 – 161 (2014)**

Recovery of Indium(III) from a Hydrochloric Acid Medium with Two Types of Solvent Impregnated Resins Containing Sec-octylphenoxy Acetic Acid

Haimei LI,[1,2] Junshen LIU,[1]* Lili ZHU,[1] Xuezhen GAO,[1] Shilong WEI,[1] Lei GUO,[1]
Shengxiao ZHANG[1] and Xunyong LIU[1]
[1]School of Chemistry & Materials Science, Ludong University, Yantai 264025, P. R. China
[2]Department of Management Engineering, Yantai Engineering & Technology College, Yantai 264025, P. R. China
(Received November 1, 2013; Accepted February 26, 2014)

A solvent impregnated resin (SIR) with sec-octylphenoxy acetic acid (CA-12) impregnated on a styrene-divinylbenzene copolymer support (HZ818) was first prepared. To improve the stability of the first SIRs for indium adsorption, a novel type of SIR (NSIR) had been prepared by forming a PVA–boric acid protective layer on the first SIR containing CA-12. The NSIR and SIR were characterized, and their adsorption behavior for indium(III) were compared by batch and column methods in a hydrochloric acid medium. Both the NSIR and SIR showed high adsorption capacities for In(III) at pH 3.0, and the maximum adsorption capacities increased with temperature. The Langmuir isotherm and pseudo second-order model fit the experiment data well at different temperatures. The NSIR showed better stability and reusability than the SIR. It is possible to separate In(III) from a mixed solution containing Zn(II), Cu(II), Cd(II) and In(III) at pH 3.0 from hydrochloric acid medium with SIR and NSIR.

1. Introduction

Indium is a rare and valuable metal that is used in a variety of industrial applications, such as liquid crystal displays (LCDs), semiconductors, low-temperature solders, infrared photodetectors, and solar cells. However, there are no discrete reserves of indium, and its global distribution is very sparse [1]. Therefore, it has to be recovered as a byproduct from other metallurgical processes or from secondary raw materials. Most commonly indium is associated with zinc, lead, copper, and tin ores [2]. Solvent extraction or ion exchange processes have been employed in the extraction of indium [3-9]. However, the main drawback of the solvent extraction process is the loss of extractant into the aqueous solution, which may cause environmental hazards and economic limitations [10]. Compared with solvent extraction, ion exchange is much simpler. Nonetheless, the low selectivity and slow adsorption and desorption rates for metal ions are its main problems.

Solvent impregnated resins (SIRs) can be considered as alternative adsorbents since they are similarly capable of selective sorption. SIRs comprising a polymeric matrix and an impregnated liquid extractant, are relatively easily to prepare. They combine the unique features and advantages of liquid-liquid extraction and ion exchange [11-13]. In SIRs, a soluble complexant (including an inert organic solvent acting as a diluent, if necessary) is sorbed into a porous polymer matrix by an

impregnation technique [13].

In previous papers, we investigated the adsorption and separation properties for indium with SIRs containing 2-ethylhexylphosphoric acid mono-2-ethylhexyl ester [14]. However, the present extractants used in SIRs for indium adsorption have some disadvantageous features, such as low adsorption capacity, toxicity and high costs. Therefore, an alternative extractant for use in SIRs for extracting indium is required. Sec-octylphenoxy acetic acid (CA-12) as a novel carboxylic acid is cheap and non-toxic, and easy to synthesize. Furthermore, CA-12 has good chemical stability, a stable composition, low aqueous solubility and little emulsification during extraction. The applications of CA-12 in the extraction of rare metals have been investigated [7,15-18]. Recently, we used CA-12 as the extractant in preparing SIRs by impregnation on modified styrene-divinylbenzene copolymer supports (HZ818) to increase the adsorption capacity for indium [19]. The maximum adsorption capacity increased by over 20% by using CA-12 [19] compared with organophosphorus compounds [14].

Sometimes, leakage of the extractant from the polymeric support may be found for SIRs, which results in the gradual loss of SIR capacity and the shortening of its life time. In order to prevent extractant loss from SIRs, different approaches have been applied to stabilize the adsorption capacities of SIRs [20-22]. In this paper, a solvent impregnated resin (SIR) with sec-octylphenoxy acetic acid (CA-12) impregnated on a HZ818 support was first prepared. To improve the stability of the first SIR for indium adsorption, it was coated with a PVA–boric acid protective layer, to form the SIR (NSIR). The adsorption and elution behavior of In(III) from hydrochloric acid solution by the SIR and NSIR were investigated by both batch and dynamic methods.

2. Experimental

2.1 Materials

Sec-octylphenoxy acetic acid (CA-12) was supplied by Shanghai Rare-earth Chemical Co., Ltd, China. Its purity is approximately 95%. The CA-12 molecular structure is shown in Figure 1.

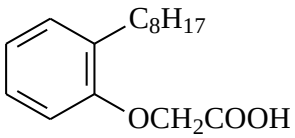

Figure 1. The molecular structure of CA-12.

Poly (vinyl alcohol) (PVA) with a polymerization degree of 1750±50 was purchased from Shanghai Aibi Chemical Co., Ltd, China. HZ818 support (styrene-divinylbenzene copolymer) was obtained from Shanghai Huazhen Polymer Co., Ltd, China. The specific surface area and pore volume of porosity for the adsorbents are 718.8 m^2/g and 1.66 mg/L, respectively. The average particle size is 0.45 mm with a mean pore size of 4.56 nm. All other chemicals used in this work are of analytical reagent grade, and were used without any further purification.

The concentration of indium in single component solutions was determined spectrophotometrically using a UV–2550 spectrophotometer (Shimadzu, Japan), and the concentration of indium in mixed component solutions was determined with an ICPE-9000 multitype ICP emission spectrometer (Shimadzu, Japan).

2.2 Preparation of SIRs and NSIRs

Before impregnation, the HZ818 support was kept in ethanol for 4 h, and washed with 5%

hydrochloric acid solution to remove inorganic impurities and monomeric material. The support was then rinsed thoroughly with distilled water to eliminate chloride ions.

The SIRs were prepared using a dry impregnation method. A known amount of the HZ818 support was placed in 50 mL of a CA-12–n-heptane solution. The mixture was stirred for 48 h at 313 K. Then the SIRs were separated from the mixed solution and the solvent removed by evaporation at 333 K in a vacuum oven.

The NSIRs were prepared in the following way: a known amount of the SIRs was immersed in 50 mL of 3% PVA –0.06% sodium alginate (w/w) solution and shaken for 22 h at 313 K. After that, the resins were separated from the solution. Then, the beads were re-immersed in a solution consisting of saturated boric acid and shaken for 8 h, and the NSIRs were obtained by a cross-linking reaction between PVA and boric acid. The beads were separated and washed with distilled water subsequently. Finally, the solvent was removed from the NSIRs by evaporation at 333 K .

The extractant investigated in this study is an acid type. Therefore, the amount of impregnated extractant was determined by washing a known amount of resin with ethanol, which can completely elute the extractant. The content of the extractant was determined by titration with an NaOH solution. A calibration curve of the extractant titration with the NaOH solution was established to determine the amount of extractant [23]. The extractant content of the SIRs and NSIRs are 2.10 and 1.81 mmol/g, respectively.

2.3 Characteristics of SIRs and NSIRs

The shapes and surface morphology of samples were examined using a scanning electron microscope (SEM), JSF5600LV, JEOL, Japan. Infrared spectra were recorded on a Nicolet MAGNAIR 550 (series II) spectrophotometer. Test conditions: potassium bromide pellets, scanning 32 times, a resolution of 4 cm^{-1}. The data were treated using Thermo Nicolet Corporation OMNIC32 software, version 6.0 a. Thermogravimetry analysis was performed on a Netzsch TG 209 thermal analyzer, using 20–30 mg of the sample under nitrogen at a heating rate of 10 K/min.

2.4 Batchwise adsorption

A 25 mL metal ion solution of known concentration was placed in a 100 mL glass-stoppered flask and the pH was adjusted to the desired value by adding an appropriate amount of hydrochloric acid solution or sodium hydroxide solution. Then, a known amount of resin was introduced and the mixture in the flask was shaken until equilibrium in a thermostatic bath. After filtration, the equilibrium pH was measured. The concentration of metal ions in the aqueous phase was analyzed. The amount of metal ions adsorbed by the resin was determined from the mass balance. The adsorption capacity Q (mg/g) was calculated using the following equation:

$$Q = \frac{(C_0 - C_e)V}{M} \quad (1)$$

where C_0 and C_e represent the initial and equilibrium concentrations (mg/L) of metal ion in the aqueous solution and V and M are the volume of the aqueous solution (mL) and the weight of resins used (mg), respectively[24].

2.5 Column adsorption

The column was prepared by placing 300 mg of resin in an empty glass column (150 mm×3.0 mm

i.d). In order to avoid resin loss, a small amount of absorbent cotton was plugged at both sides of the column before the sample solution was passed through the column. SIRs and NSIRs were first washed with HCl solution of pH 3.0 to reach the suitable pH before use. The pH of the indium(III) feed solution was also 3.0. Then the metal ion solution was fed into the column. The concentrations of the effluent samples were determined at appropriate time intervals. The saturated capacity of the resins was calculated on the basis of the total amount of metal adsorbed until the effluent concentration reached the feed concentration.

3. Results and Discussion

3.1 Characterization of SIRs and NSIRs

3.1.1 Scanning Electronic Microscopy (SEM)

The appearance and morphology of the SIRs and NSIRs was examined using scanning electron microscopy. Figure 2 shows that the protective layer changes the morphology of the beads. Figure 2 (a) shows the SIR obtained from HZ818 and CA-12. The bead has a smooth surface appearance. Figure 2 (b), (c) and (d) show different surface morphologies for the coated beads produced by cross-linking reaction of PVA and boric acid. The surface of perfect NSIRs has a distinct "skin" compared with the SIRs. This provides a protective barrier on the SIRs to prevent the loss of the extractant from the internal pore structure of the SIRs to the external aqueous phase.

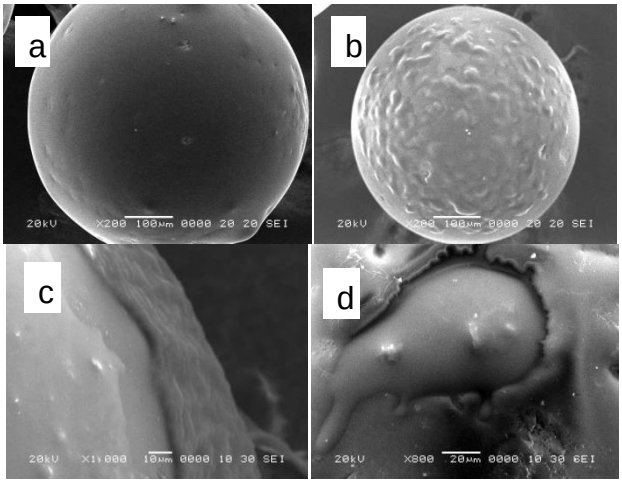

Figure 2. SEM photographs of SIRs (a), NSIRs (b, c and d).

3.1.2 Thermogravimetry (TG)

The thermal stability of two types of resins was established by thermogravimetry analysis. Their thermogram curves are shown in Figure 3. The HZ818 support was used as the reference material. The weight loss of HZ818 started at 350 ℃, which means that HZ818 has good thermal stability and can be used as the matrix material.

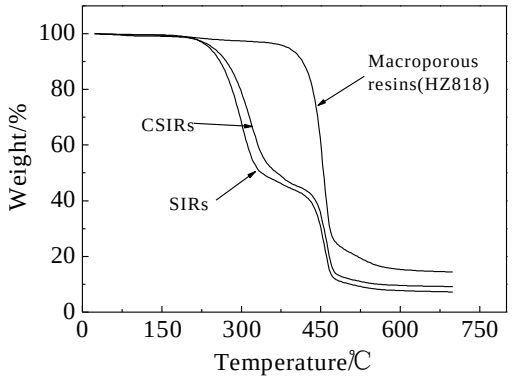

Figure 3. TGA of the HZ818 support, SIRs and NSIRs.

The weight loss between 230 ^{o}C and 320 ^{o}C for SIRs and NSIRs is due to the fracture of the organic chain of the impregnated extractant. The weight losses in this temperature range were about 57.2% and 52.2% for SIRs and NSIRs, respectively. Therefore the extractant content in the pore structures of the SIRs and NSIRs was calculated to be 2.06 mmol/g for the SIRs and 1.88 mmol/g for the NSIRs, respectively. These results were consistent with the results of acid base titration experiments (section 2.2).

In addition, the extractant amount for the NSIRs is slightly lower than that for the SIRs because of the added weight of the PVA–boric acid protective layer in the NSIRs. The second obvious mass loss is observed from 340 ^{o}C with both resins, which results from the decomposing of the matrix material HZ818. The thermal stability indicated that the two types of resins could meet the requirements for adsorbing metal ions.

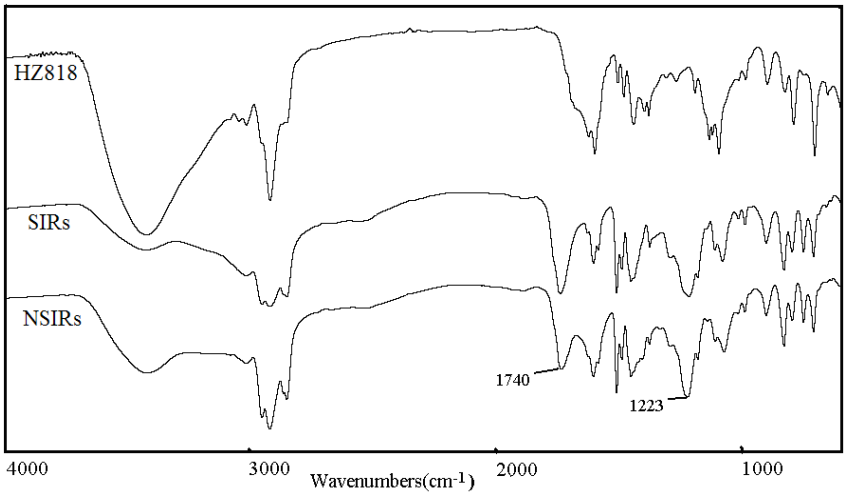

Figure 4. FTIR spectra of the HZ818 support, SIRs and NSIRs.

3.1.3 Fourier transform infrared spectra (FTIR)

Fourier transform infrared spectra can provide a qualitative and preliminary analysis of the main functional groups in the adsorbents. Figure 4 shows a FTIR profile for both the SIRs and NSIRs. The peak representing the C=O stretching frequency for the carboxylic acid appears at 1740 cm^{-1}, and the band peak for O-H is found at 1223 cm^{-1}. There was no change in the characteristic peaks before and after the coating cross-linking reaction. As can be seen, there was no influence on the nature of the extractant due to the coating procedure.

3.2 Bathwise adsorption properties of In(III)

3.2.1 Effect of pH on adsorption

The influence of pH on the adsorption performance of In(III) with both the SIRs and NSIRs was investigated by varying the initial solution pH (keeping other parameters constant). Figure 5 (A) shows the adsorption results. The adsorption capacities for In(III) with two types of SIRs increased gradually with increasing pH from 1.5 to a maximum value (pH 3.2), indicating that the adsorption of In(III) ions progresses via a cation exchange reaction[24]. The capacities did not chang much beyond pH 3.2 under the experimental conditions. This means that the nature of the extractant for In(III) adsorption changed little before and after coating. This result was consistent with the infrared analysis. In addition, because the surface protective layer causes a relative decrease in extractant content of the NSIRs, the adsorption capacities of the NSIRs were a little lower than that of the SIRs.

Figure 5 (B) shows the effect of equilibrium pH on adsorption. The adsorption curves were similar to that of Figure 5 (A), while only shifted slightly to lower pH values because of the hydrogen ions release via the cation exchange reaction.

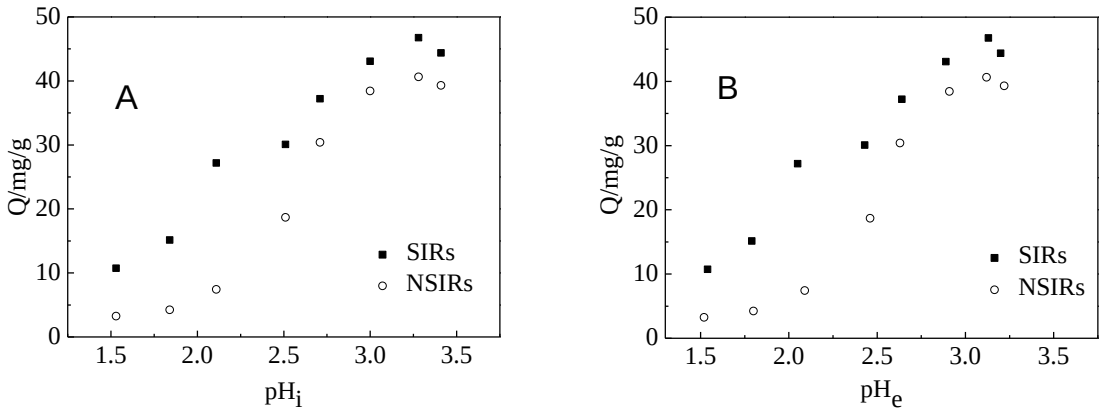

Figure 5. Effect of solution pH on In(III) adsorption with SIRs and NSIRs. (A) initial solution pH (pH_i); (B) equilibrium solution pH (pH_e); Experiment condition: V = 25 mL, m = 25 mg, T=25 ^oC, C_0 = 60 mg/L

3.2.2 Adsorption isotherms

For interpretation of the isothermal adsorption experimental data, Langmuir and Freundlich isotherm models were used [25]. The Langmuir model assumes that the uptake of metal ions occurs on a homogeneous surface by monolayer adsorption without any interaction between adsorbed ions. The Freundlich model assumes that the uptake or adsorption of metal ions occurs on a heterogeneous surface by multilayer adsorption. The Langmuir (2) and Freundlich (3) models can be represented in a linearized form as

$$\frac{C_e}{Q} = \frac{1}{Q_0 K_L} + \frac{C_e}{Q_0} \quad (2)$$

$$\log Q = \log K_F + \frac{1}{n}\log C_e \quad (3)$$

where Q is the adsorption capacity, mg/g; C_e is the equilibrium concentration of In(III), mg/L; Q_o is the saturated adsorption capacity, mg/g; K_L is an empirical parameter; n is Freundlich constant and K_F is the binding energy constant reflecting the affinity of the adsorbents to metal ions. The adsorption data for the Langmuir and Freundlich isotherm models along with the regression coefficients (R^2) with SIRs and NSIRs for In(III) are shown in Table 1.

As seen from Table 1, the R^2 values indicate that the Langmuir isotherm fits the experimental data better than the Freundlich isotherm at different temperatures. This fact shows that the two types of adsorbents prepared by different methods have similar mechanisms and both of them exhibit monolayer adsorption [25].

Table 1. Freundlich and Langmuir constants for In(III) adsorption with SIRs and NSIRs

Experiment condition: V = 25 mL, m= 25 mg, T=25 ^{o}C, pH_e=3.05±0.05

Resins	T (K)	Freundlich isotherm			Langmuir isotherm		
		K_F (mg/g)	n	R^2	Q_0 (mg/g)	K_L (L/mg)	R^2
SIRs	288	8.76	3.61	0.816	33.3	0.134	0.996
	298	10.8	3.09	0.667	48.7	0.136	0.994
	308	13.9	3.22	0.588	59.5	0.119	0.991
	318	18.5	3.28	0.602	71.7	0.184	0.993
NSIRs	288	5.08	2.72	0.787	31.9	0.063	0.993
	298	10.3	3.29	0.675	42.5	0.150	0.994
	308	13.0	3.36	0.564	53.6	0.112	0.993
	318	13.7	3.06	0.688	63.4	0.108	0.994

3.2.3 Adsorption thermodynamics

The effect of temperature on the adsorption of indium (III) using the SIRs and NSIRs was investigated from 15 to 45℃ (288–318 K). The experiments were carried out with 0.025 g of the SIR or NSIR of a contact time of 24 h and a liquid/**s**olid ratio of 1 (L/g). The equilibrium constant is expressed by equation [25]:

$$K_c = \frac{C_{Ae}}{C_e} \tag{4}$$

where K_c is the distribution coefficient, C_{Ae} (mg/L) is the equilibrium concentration of In(III) on the adsorbent, C_e (mg/L) is the equilibrium concentration of In(III) in solution.

Thermodynamic parameters such as free energy change (ΔG), enthalpy change(ΔH) and entropy change(ΔS) can be calculated by following equations:

$$\Delta G = -RTLnK_c \tag{5}$$

$$\Delta G = \Delta H - T\Delta S \tag{6}$$

$$LnK_c = -\frac{\Delta H}{RT} + \frac{\Delta S}{R} \tag{7}$$

where R is the universal gas constant (8.314 J·mol^{-1}·K^{-1}) and T is the absolute temperature (K). The values of ΔH and ΔS were calculated from the intercepts and slopes of the straight line plots of LnK_c *vs*. 1/T (Figure 6) and are given in Table 2.

The positive values of the enthalpy change (ΔH) indicate an endothermic adsorption process. The positive entropy value (ΔS) may be related to the increased randomness at the solid-solution interface due to the adsorption of In(III) [26,27]. The negative values of ΔG confirm the feasibility of the adsorption process of In(III) on NSIRs at 298 K, 308 K, 318 K, as expected for a spontaneous process. The decrease in ΔG with the increase in temperature indicates more efficient adsorption at higher temperatures. These results are consistent with the adsorption of In(III) on modified solvent impregnated resins containing CA-12, reflecting the nature of the extractant (CA-12) impregnated on the resin.

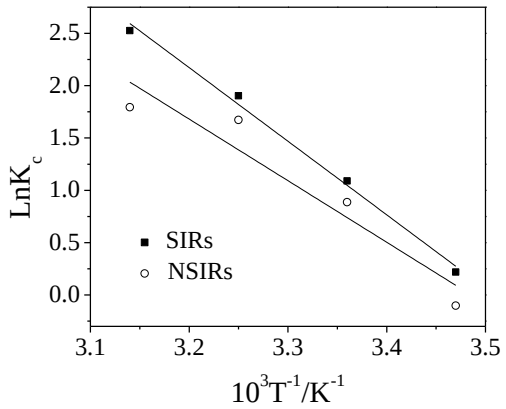

Figure 6. Plots of LnK_c vs 1/T for In(III) adsorption with SIRs and NSIRs.
Experiment condition: V = 25 mL, m = 25 mg, T=25 ^oC, pH_e=3.05±0.05

Table 2. Thermodynamic Parameters for In(III) adsorption with SIRs and NSIRs

Resins	T(K)	ΔG (kJ/mol)	ΔH (kJ/mol)	ΔS (J·mol^{-1}·K^{-1})
SIRs	288	-0.052	58.5	205.1
	298	-2.700		
	308	-4.872		
	318	-6.676		
NSIRs	288	0.025	48.9	170.6
	298	-2.198		
	308	-4.285		
	318	-4.742		

However the value of ΔG is positive for the NSIRs at 288K. Similar phenomena were found in the adsorption of Hg(II) on chitosan-coated cotton fibers[26], and Ag(I) on amidoximated porous acrylonitrile/methyl acrylate copolymer beads[27], which was attributed to the presence of an energy barrier in the adsorption process and to the activated complex in the transition state in an excited form.

3.2.4 Adsorption kinetics

The kinetics of adsorption that describes the solute uptake rate which governs the contact time for the adsorption reaction is one of the important characteristics that define the efficiency of adsorption. Hence, in the present study, the kinetics of In(III) removal was determined to understand the adsorption behavior of the SIRs and NSIRs at different temperatures (Figure 7).

It can be seen from Figure 7 that, with increasing temperature, the adsorption rate of In(III) for the two types of resins gradually increased. The adsorption rate for In(III) with the NSIRs is similar to that for the SIRs. The Lagergren first order kinetics model and a pseudo second order model were used to investigate the dominant mechanism of the adsorption process. The Lagergren first order model is

represented by the equation:[26]

$$\log(Q_e - Q_t) = \log Q_e - \frac{k_1}{2.303} t \quad (8)$$

where Q_e is the amount of adsorbed In(III) at equilibrium (mg/g), Q_t is the amount of adsorbed In(III) at time t (mg/g), and k_1 is the Lagergren first order rate constant (min^{-1}). The calculated parameters are presented in Table 3.

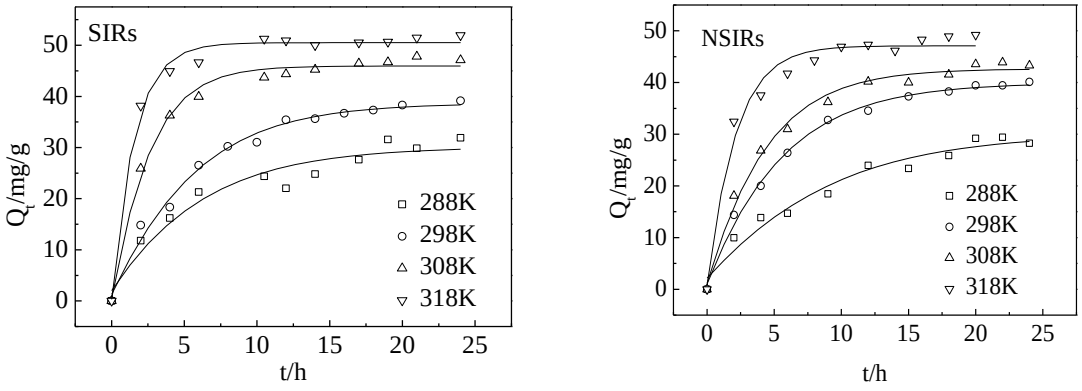

Figure 7. Effect of contact time on In(III) adsorption at different temperatures.
Experimental conditions: pH_i = 3.0, V = 25 mL, m = 25 mg, C_0 = 60 mg/L.

Table 3. Calculated parameters for the kinetic models for In(III) adsorption with SIRs and NSIRs

Resins	T (K)	$Q_{e.exp}$ (mg/g)	Legergren-first-order model			pseudo-second-order model		
			$Q_{e,cal}$ (mg/g)	k_1 (min^{-1})	R^2	$Q_{e,cal}$ (mg/g)	k_2 (g/mg min)	R^2
SIRs	288	31.9	33.2	0.1521	0.6690	37.9	0.0047	0.9621
	298	39.1	39.2	0.1798	0.9780	47.9	0.0041	0.9928
	308	47.8	25.0	0.1679	0.9882	51.1	0.0111	0.9995
	318	51.9	13.3	0.1468	0.8751	53.3	0.0230	0.9997
NSIRs	288	29.4	42.9	0.1876	0.7075	37.9	0.0034	0.9649
	298	40.1	42.5	0.1878	0.9802	48.9	0.0040	0.9977
	308	43.9	41.7	0.1937	0.8866	50.3	0.0056	0.9984
	318	49.1	29.7	0.2369	0.9782	52.5	0.0131	0.9987

It was observed that the adsorption of In(III) at different temperatures did not fit the Lagergren first order model. The kinetic data were further analyzed using a pseudo second order model, and the linear form of this model is shown as follows [26]:

$$\frac{t}{Q_t} = \frac{1}{h} + \frac{1}{Q_e} t \quad (9)$$

where the initial adsorption rate h (mg/g min) is given by $h = k_2 Q_e^2$, and k_2 is the rate constant of the pseudo second order equation (g/mg $min^{1/2}$). The calculated parameters are also presented in Table 3. It can

be observed from Table 3 that the pseudo second order model fitted the data well with a good linearity over the entire investigation, because the values of the correlation coefficients (R^2) for equation (8) were very high. Also the theoretical Q_e values calculated from the pseudo second order model were more in accordance with the experimental values than the Lagergren first order model with the two types of resins. Therefore, it was appropriate to use the pseudo second order kinetic model to predict the adsorption kinetics of the studied ions.

According to Reichenberg [28] and Boyd et al. [29], the adsorption procedure of the SIRs for metal ions takes place through two diffusion mechanisms, film diffusion and particle diffusion. Film diffusion is the rate–controlling step when the concentration of metal ions is low, particle diffusion could be the rate–controlling step while the concentration of metal ions is high.

The kinetic data were analyzed by the diffusion mechanism model given by Reichenberg [28] and Helfferich [30]. The following equations were used:

$$F(t) = \frac{Q_t}{Q_0} = 1 - \frac{6}{\pi^2} \sum_{n=1}^{\infty} \frac{1}{n^2} \exp(-\frac{\overline{D} t \pi^2 n^2}{r_0^2}) \tag{10}$$

or

$$F(t) = 1 - \frac{6}{\pi^2} \sum_{n=1}^{\infty} \frac{1}{n^2} \exp(-n^2 Bt) \tag{11}$$

$$B = \frac{\overline{D} \pi^2}{r_0^2} \tag{12}$$

where $F(t)$ is the degree of ion exchange at time t, Q_t and Q_0 are the adsorption capacity at time t and equilibrium respectively (mg/g), $\overline{D}$ is the effective diffusion coefficient of indium ions in the adsorbent particle, r_0 is the radius of the adsorbent particle, and n is an integer that defines the infinite series solution. The Bt values were obtained from the corresponding values of $F(t)$. The Bt values for each $F(t)$ value were given by Reichenberg [28].

The linear plots of Bt versus t are shown in Figure 8, and the linear equations and correlation coefficients are shown in Table 4. If the plot was a straight line passing through the origin, the adsorption process should be governed by the particle diffusion mechanism, otherwise it might be dominated by the film diffusion mechanism. As shown in Figure 8 and Table 4, all the lines of the linear plots did not pass through the origin under the experimental conditions, suggesting that film diffusion dominated the adsorption process.

Table 4. The *Bt* vs. *t* Linear equations and R^2 coefficients

Adsorbent	Temperature (K)	Linear equation	R^2
SIRs	288K	*Bt*=0.080*t*+0.015	0.888
	298K	*Bt*=0.172*t*-0.373	0.966
	308K	*Bt*=0.168*t*+0.181	0.992
	318K	*Bt*=0.139*t*+0.905	0.844
NSIRs	288K	*Bt*=0.095*t*-0.153	0.935
	298K	*Bt*=0.171*t*-0.364	0.973
	308K	*Bt*=0.143*t*-0.055	0.977
	318K	*Bt*=0.201*t*+0.194	0.936

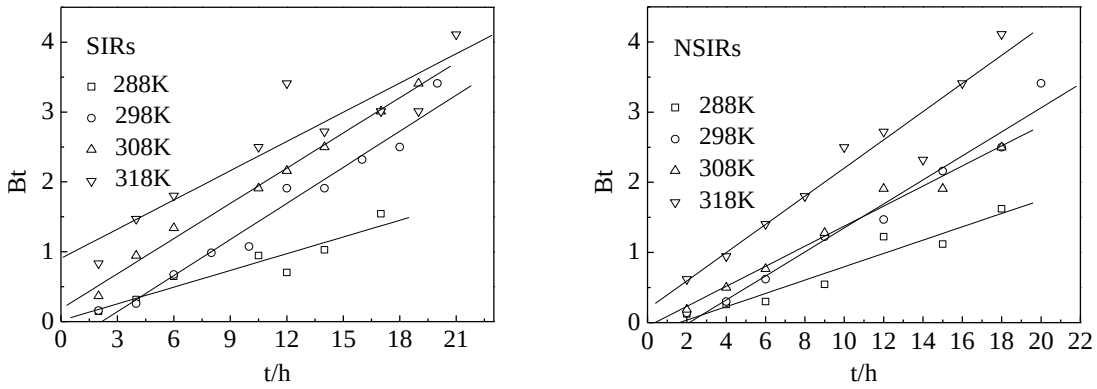

Figure 8. Plots of *Bt* vs. *t* for the adsorption of In(III) with SIRs and NSIRs.

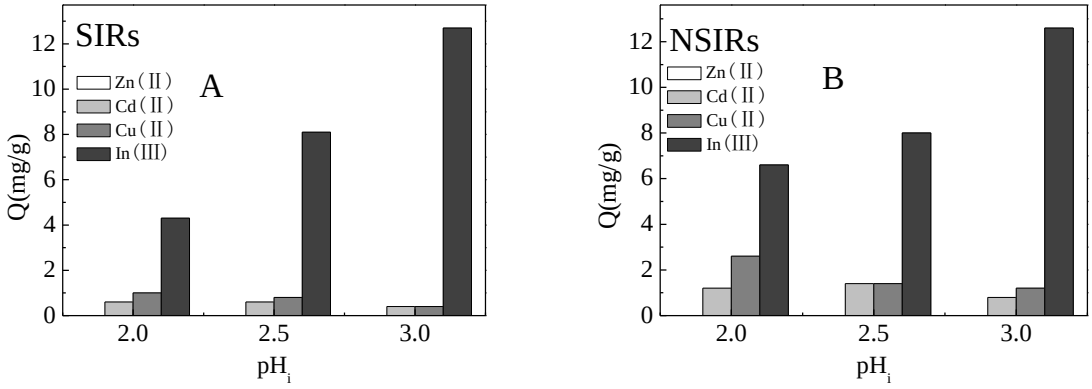

Figure 9. Influence of the composition of the solution on In(III) adsorption

(A) influence of the presence of Zn(II), Cu(II), Cd(II) at different pH_i with SIRs;

(B) influence of the presence of Zn(II), Cu(II) and Cd(II) at different pH_i with NSIRs.

3.2.5 The effects of competing metal ions

The recovery of indium was investigated from copper smelter flue dust containing various metals,

such as zinc, copper, indium, cadmium, et al [31]. Hence the selective adsorption of In(III) from a mixed HCl solution containing Zn(II), Cu(II), Cd(II) and In(III) was investigated with both SIRs and NSIRs. The effects of acidity and competing metal ions on In(III) recovery were studied. The results are shown in Figure 9.

It is shown that the adsorption of In(III) increased with an increase in the initial pH. The competing anions of the other metal ions cause a decrease in the In(III) adsorption since their anionic species compete for the same binding sites. Zn(II) was not adsorbed in the range of acid concentration studied with both SIRs and NSIRs. This is probably due to the fact that Zn(II) does not form anionic complexes with chloride ions. Its charge is not favorable for electrostatic attraction/ion exchange [32]. The presence of other metals such as Cu(II) and Cd(II) in the mixed solution hardly interfere with In(III) adsorption at an initial pH=3.0 with SIRs and NSIRs. Hence, it is possible to separate In(III) from a mixed solution containing Zn(II), Cu(II), Cd(II) and In(III) in hydrochloric solution at an initial pH=3.0 with the SIRs and NSIRs.

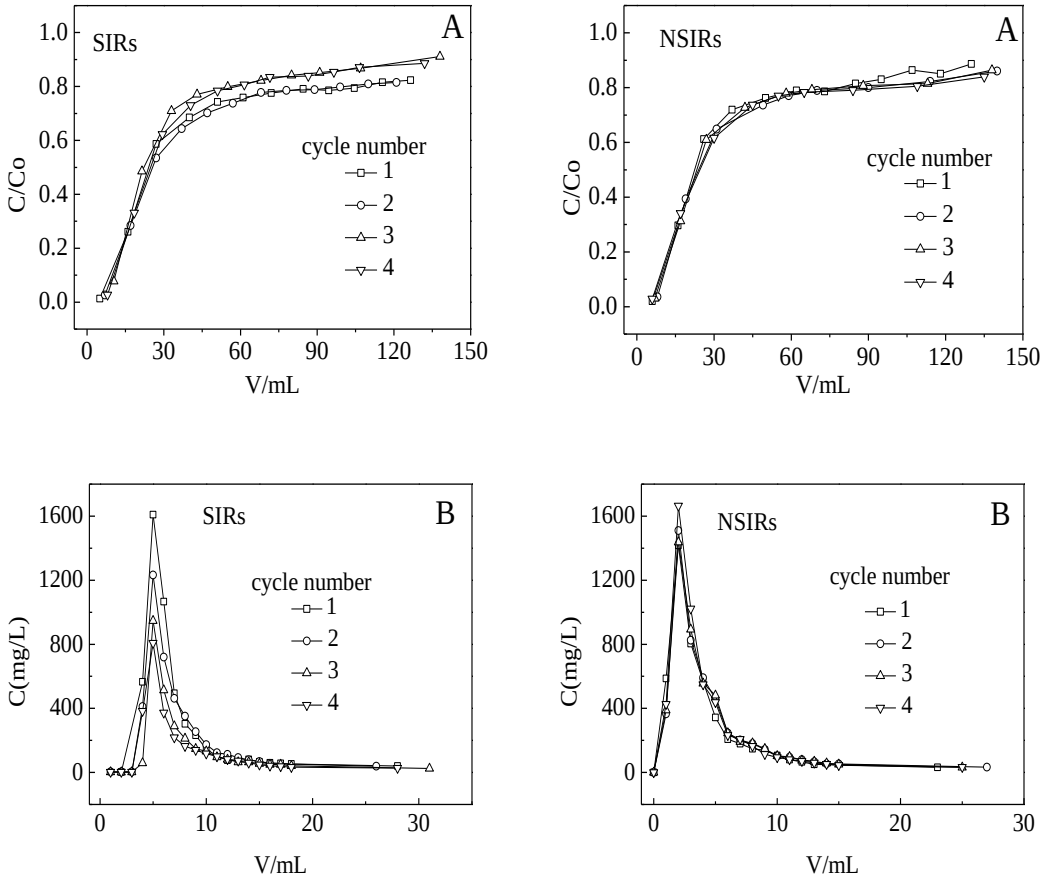

Figure 10. Recycle tests with the SIRs and NSIRs. (A) Comparison of breakthrough curves of SIRs and NSIRs after several resin bed adsorption-elution cycles: m = 300 mg, 150 mm×3.0 mm i.d.; sample flow rate, 1.0 mL/min; loading solution, C_{In} = 90 mg/L, pH_i = 3.0; (B) Comparison of elution curves for the SIRs and NSIRs after several resin bed adsorption-elution cycles : m = 300 mg, 150 mm×3.0 mm i.d.; elution rate, 1.2 mL/min; loading solution, C_{HCl} = 2.0 mol/L.

3.3 Recycle Test

The recycle performances of the SIRs and NSIRs were investigated for several adsorption-elution cycles, respectively. Figure 10 shows the breakthrough curves and stripping curves for the SIRs and NSIRs. Table 5 shows the adsorption capacities and stripping amounts for the SIRs and NSIRs after several adsorption-elution cycles. The adsorption capacity (mg) was calculated on the basis of the total amount of metal ion adsorbed until the effluent concentration reached the feed concentration. The stripping amount (mg) was the amount of metal ions stripped from loaded SIRs to the stripping solution. The stripping efficiency (%) was calculated from equation (12).

$$\text{Stripping efficiency (\%)} = \frac{\text{amount of In(III) stripped to stripping solution}}{\text{amount of In(III) sorbed on SIRs}} \times 100 \qquad (13)$$

The breakthrough curves and stripping curves for the NSIRs in the 2-4th run were not obviously different from that in the first run (Figure 10). From Table 5, the adsorption capacity of the NSIRs in the 4th run (6.31 mg) was almostly the same as that in the first run (6.19 mg). Therefore we can conclude that the amount of the extractant contained in the NSIRs remained nearly constant, and the NSIRs were of good stability and can be considered suitable for repeated use. However, the breakthrough curves for the SIRs shifted a little from right to left as the cycle number increase (Figure 10). Also the adsorption capacities of the SIRs in the 2-4th cycles obviously decreased compared with the first run (Table 5). This may will be due to the gradual slight loss of the extractant amount contained in the SIRs. From Table 5, we can also see that the stripping efficiency was high (almost 100%), which indicated that the In(III) ion adsorbed on the two types of resins can be thoroughly stripped with 2.0 mol/L HCl solution.

Table 5. Comparison of parameters of the SIRs and NSIRs after several adsorption-elution cycles

	Cycle times	Adsorption capacity/mg	Stripping amount/mg	Stripping efficiency/%
SIRs	1	6.04	6.05	100.2
	2	4.04	4.08	101.0
	3	4.11	4.14	100.7
	4	4.41	4.40	99.8
NSIRs	1	6.19	6.18	99.8
	2	6.07	6.00	98.8
	3	6.28	6.24	99.4
	4	6.31	6.34	100.5

4. Conclusions

SIRs and NSIRs containing sec-octylphenoxy acetic acid as the extractant have high adsorption capacitise for In(III). The NSIRs prepared by formation of the PVA–boric acid protective layer are more stable, and the utilization rate of the extractant in the NSIRs is better than in the SIRs. The optimal initial

pH for the adsorption of indium was found to be 3.0 with born types of resins in the hydrochloric acid system. The Langmuir isotherm fits the experiment data well at different temperatures. Adsorption capacity increased with increasing temperature. The reaction is endothermic and the enthalpy change was close to 8.41 kJ/mol for the SIRs and 35.19 kJ/mol for the NSIRs, respectively. The kinetic data indicated that the In(III) adsorption process followed a pseudo second-order rate equation. The NSIRs have greater stability than the SIRs and can be considered suitable for repeated use. It is possible to separate In(III) from a mixed solution (Zn(II), Cu(II), Cd(II) and In(III)) at an initial pH 3 in hydrochloric acid medium with SIRs and NSIRs.

Acknowledgment

This project was supported by the National Natural Science Foundation of China (Grant No. 21171085; 21206066; 21207059; 21304043), the Natural Science Foundation of Shandong Province, China (No. ZR2010BM027, ZR2011BQ012; ZR2012BQ024). The authors also thank their colleagues and other students who participated in this work.

References

1) T. Ogi, K. Tamaoki, N. Saitoh, A. Higashi, Y. Konishi, *Biochem. Eng. J*., **63,** 129-133 (2012).
2) S. Virolainen, D. Ibana, E. Paatero, *Hydrometallurgy*, **107**, 56-61 (2011).
3) A.P. Paiva, *Sep. Sci. Technol.*, **36**,1395-1419 (2001).
4) B. Gupta, N. Mudhar, I. Singh, *Sep. Purif. Technol*., **57**, 294-303 (2007).
5) M.S. Lee, J.G. Ahn, E.C. Lee, *Hydrometallurgy*, **63**, 269-276 (2002).
6) S. Nishihama, T. Hirai, I. Kom*asawa, Ind. Eng. Chem. Res., 38, 1032-1039 (1999).*
7) X. Zhang, G. Yin, Z. Hu, *Talanta*, **59**, 905-912 (2003).
8) A.W. Trochimczuk, S. Czerwińska, *React. Funct. Polym.*, **63**, 215-220 (2005).
9) M.C.B. Fortes, A.H. Martins, J.S. Benedetto, *Miner. Eng.*, **16**, 659-663 (2003).
10) M.P. Gonzalez, I. Saucedo, R. Navarro, M. Avila, E. Guibal, *Ind. Eng. Chem. Res.*, **40**, 6004-6013 (2001).
11) N. Kabay, J.L. Cortina, A. Trochimczuk, M. Streat, *Reat. Funct. Polym.*, **70**, 484-496 (2010).
12) K. Onishi,T. Nakamura,S. Nishihama, K. Yoshizuka, *Ind.Eng. Chem.Res.* **49**, 6554–6558 (2010).
13) T. Kitabayashi, T. Sana, S. Kiyoyama, T. Takei, M. Yoshida, K. Shiomori, *Solvent Extr. Res. Dev., Jpn.*, **20**, 137-147 (2013).
14) Y. Yuan, J. Liu, B. Zhou, S. Yao, H. Li, W. Xu., *Hydrometallurgy*, **101**, 148-155 (2010).
15) M. Tian, N. Song, D. Wang, X. Quan, Q. Jia, W. Liao, L. Lin, *Hydrometallurgy*, **111-112**, 109-113 (2012).
16) X. Zhang, X. Lou, G. Yin, Y. Zhang, *Rare metals*, **23**, 6-9 (2004).
17) W. Li, X. Wang, S. Meng, D. Li, Y. Xiong, *Sep. Purif. Technol.*, **54**, 164-169 (2007).
18) H. Ma, Y. Lei, Q. Jia, W. Liao, L. Lin, *Sep. Purif. Technol.*, **80**, 351-355 (2011).
19) H. Li, J. Liu, X. Gao, C. Liu, L. Guo, S. Zhang, X. Liu, C. Liu, *Hydrometallurgy*, **121-124**, 60-67 (2012).
20) D. Muraviev, L. Ghantous, M.Valiente, *React. Funct. Polym.*, **38**, 259-268 (1998).

21) A.W. Trochimczuk, N. Kabay, M. Arda, M. Streat, *React. Funct. Polym.*, 59, 1-7 (2004).
22) N. Kabay, J. L. Cortina, A. Trochimczuk, M. Streat, *React. Funct. Polym.*,**70**,484-496(2010).
23) J.H. Chen, W.R. Chen, Y.Y. Gau, C.H. Lin, *React. Funct. Polym.*, **56**, 175-188 (2003).
24) S.Nishihama, K.Kohata, K.Yoshizuka, *Sep. Purif. Technol.*, **118**, 511-518 (2013).
25) N. V. Nguyen, J. Lee, J. Jeong, B.D.Pandey, *Chem. Eng. J.*,**219**,174–182 (2013).
26) R. Qu, C. Sun, F. Ma, Y. Zhang, C, Ji, Q. Xu, C. Wang, H. Chen, *J. Hazard. Mater.*, **167**, 717-727 (2009).
27) X. Liu, H. Chen, C. Wang, R. Qu, C. Ji, C. Sun, Q. Xu, *Polym. Advan. Technol.*, **22**, 2032-2038 (2011).
28) D. Reichenberg, *J. Am. Chem. Soc.*, **75**, 589-597 (1953).
29) G.E. Boyd, A.W. Adamson, L.S. Myers, *J. Am. Chem. Soc.*, **69**, 2836-2848 (1947).
30) Y. Zhang, R. Qu, C. Sun, C. Wang, C. Ji, H. Chen, P. Yin, *Appl. Surf. Sci.*, **255**, 5818 (2009).
31) J.J. Ke, R.Y. Qiu, C.Y. Chen, *Hydrometallurgy*, **12**, 217-224 (1984).
32) A. Arias, I. Saucedo, R. Navarro, V. Gallardo, M. Martinez, E. Guibal, *React. Funct. Polym*., **71**, 1059-1070 (2011).